NeuroImage 256 (2022) 119221

Contents lists available at ScienceDirect

NeuroImage

journal homepage: www.elsevier.com/locate/neuroimage

# The dorsal premotor cortex encodes the step-by-step planning processes for goal-directed motor behavior in humans

Yoshihisa Nakayama[a,b,*], Sho K. Sugawara[a,c], Masaki Fukunaga[c,d], Yuki H. Hamano[c], Norihiro Sadato[c,d], Yukio Nishimura[a]

[a] Neural Prosthetics Project, Tokyo Metropolitan Institute of Medical Science, Kamikitazawa 2-1-6, Setagaya, Tokyo 156-8506, Japan
[b] Frontal Lobe Function Project, Tokyo Metropolitan Institute of Medical Science, Setagaya, Tokyo 156-8506, Japan
[c] Division of Cerebral Integration, National Institute for Physiological Sciences, Okazaki, Aichi 444-8585, Japan
[d] Department of Physiological Sciences, SOKENDAI (The Graduate University for Advanced Studies), Hayama, Kanagawa 240-0193, Japan

ARTICLE INFO

*Keywords:*
Premotor cortex
Action
Goal
Visuomotor behavior
Visuo-goal mapping
fMRI

ABSTRACT

The dorsal premotor cortex (PMd) plays an essential role in visually guided goal-directed motor behavior. Although there are several planning processes for achieving goal-directed behavior, the separate neural processes are largely unknown. Here, we created a new visuo-goal task to investigate the step-by-step planning processes for visuomotor and visuo-goal behavior in humans. Using functional magnetic resonance imaging, we found activation in different portions of the bilateral PMd during each processing step. In particular, the activated area for rule-based visuomotor and visuo-goal mapping was located at the ventrorostral portion of the bilateral PMd, that for action plan specification was at the dorsocaudal portion of the left PMd, that for transformation was at the rostral portion of the left PMd, and that for action preparation was at the caudal portion of the bilateral PMd. Thus, the left PMd was involved throughout all of the processes, but the right PMd was involved only in rule-based visuomotor and visuo-goal mapping and action preparation. The locations related to each process were generally spatially separated from each other, but they overlapped partially. These findings revealed that there are functional subregions in the bilateral PMd in humans and these subregions form a functional gradient to achieve goal-directed behavior.

## 1. Introduction

In daily life, we often select an appropriate action from multiple alternatives according to circumstances. For instance, when an individual sees a red traffic light while driving a car or riding a motorcycle, they apply the foot brake pedal or hand brake lever, respectively. This situation implies that the visual stimulus does not instruct the action itself at the physical level (e.g., direction, amplitude, speed, or effector), but creates an abstract representation of the behavior or "behavioral goal" to be performed that is independent of physical parameters. Therefore, the ability to form an arbitrary linkage between visual information and behavioral goal (visuo-goal mapping) is essential for achieving this type of behavior.

Neuropsychological evidence in human patients indicates that lesions of the premotor or parietal cortex cause ideomotor apraxia, which is a cognitive disorder characterized by the inability to take an appropriate action in accordance with an external stimulus such as performing accurate movements on verbal command and imitating others' gestures, even though the patient understands the meaning of the command or gestures and does not have aphasia or paralysis (Alexander et al., 1992; Heilman et al., 1982; Wheaton and Hallett, 2007). One interpretation of this symptom is that the disability is caused by deficits in creating conceptual knowledge for an action (Buxbaum and Randerath, 2018; Kemmerer et al., 2012; Tranel et al., 2003). Conceptual knowledge for an action is considered to be equivalent to a behavioral goal in terms of the visuo-goal paradigm; therefore, some symptoms of ideomotor apraxia can be considered as a deficit of visuo-goal behavior. From this perspective, the premotor and parietal cortices are candidate neural substrates for visuo-goal behavior.

Previous studies have revealed that the dorsal premotor cortex (PMd) plays a central role in conditional visuomotor behavior, in which a visual signal is arbitrarily linked with physical parameters (Amiez et al., 2006; Boussaoud, 2001; Boussaoud et al., 1993; Boussaoud and Wise, 1993; Cisek and Kalaska, 2005; Grafton et al., 1998; Halsband and Passingham, 1985; Kurata and Hoffman, 1994; Passingham, 1993; Petrides, 1986; Simon et al., 2002; Toni et al., 2002, 2001, 1999). However, the conventional conditional visuomotor paradigm does not examine the process of generating a behavioral

* Corresponding author at: Neural Prosthetics Project, Tokyo Metropolitan Institute of Medical Science, Kamikitazawa 2-1-6, Setagaya, Tokyo 156-8506, Japan.
*E-mail address:* nakayama-ys@igakuken.or.jp (Y. Nakayama).

https://doi.org/10.1016/j.neuroimage.2022.119221.
Received 7 December 2021; Received in revised form 13 April 2022; Accepted 15 April 2022
Available online 18 April 2022.

goal because the physical parameters of an action are uniquely specified immediately after the visual stimulus is presented. Therefore, we developed a new behavioral task for examining visuo-goal behavior in which a visual signal provides instructions for a behavioral goal rather than an action itself and examined the neuronal representation of visuo-goal planning processes. We found that PMd neurons of monkeys are involved in retaining behavioral goal information and then transforming this information into physical movement parameters (i.e., an action) (Nakayama et al., 2016, 2008).

In light of the above, the PMd may play an important role in the processes of conditional visuomotor and visuo-goal behavior. However, the similarities and differences of the neural representations of the behavioral processes underlying visuomotor and visuo-goal behavior are unknown. In addition, it is unknown which components of the visuomotor and visuo-goal planning processes the PMd and other areas are involved in. Here, we assume three separate planning processes in terms of visuomotor and visuo-goal behavior. In visuomotor behavior, we first map a visual stimulus onto an action in a rule-based manner (rule-based visuomotor mapping). Then, we specify an action plan and maintain it, regardless of whether or not the action is taken after a certain period (action plan specification). Finally, we decide to perform the action and prepare the action before the appropriate time (action preparation). Conversely, in visuo-goal behavior, we first map a visual stimulus onto a goal in a rule-based manner (rule-based visuo-goal mapping). Thereafter, we transform the goal plan into an action plan (transformation of a goal into an action). Finally, as with visuomotor behavior, we prepare the action before the appropriate time (action preparation).

In the present study, we created a new behavioral task for humans, in which visual signals indicate an action or behavioral goal, and directly compared the step-by-step neural processes for achieving visuo-goal and visuomotor behavior. By comparing the conditions in different task stages, we could dissociate the processes for rule-based visuomotor mapping and visuo-goal mapping, action plan specification, transforming a goal into an action, and action preparation. We examined whole-brain activity related to the processes for goal-directed motor behavior in humans using event-related functional magnetic resonance imaging (fMRI). We found strong evidence that there are subregions in the bilateral PMd that make a functional gradient to achieve visuomotor and visuo-goal behavior.

## 2. Materials and methods

### 2.1. Participants

Twenty-nine healthy right-handed normal adult volunteers participated in the present study. Handedness was assessed with the Edinburgh Handedness Inventory (Oldfield, 1971). All participants were native Japanese speakers, and all of the instruction messages for the behavioral task (Fig. 1A and B) were written in Japanese. None of the participants had a history of neurological or psychiatric disease. All participants gave written informed consent for participation in the experiment, and the study was conducted according to the Declaration of Helsinki and approved by the Ethics Committees of Tokyo Metropolitan Institute of Medical Science (approval nos. 17-3 and 20-6) and the National Institute for Physiological Sciences (approval nos. 17A042, 18A005, 19A005, and 20A008). One of the participants was excluded from the following analyses because their rate of correct responses was substantially low (see also Table S1). Finally, data from 28 individuals (13 females and 15 males, 22.1 ± 3.1 years old) were analyzed.

### 2.2. Apparatus

A digital light processing projector (EH503; Optoma, New Taipei City, Taiwan) was placed outside and behind the MRI scanner and projected visual stimuli through another waveguide to a translucent screen that the participant viewed via a mirror attached to the head coil of the scanner. The distance between the screen and the participant's eye was approximately 48 cm and the visual angle was 5.2º (horizontal) × 3.9º (vertical). Responses were measured using an MRI-compatible joystick (Current Designs, Philadelphia, PA). Presentation 18.3 software (Neurobehavioral Systems, Berkeley, CA) and a personal computer (dc7900; Hewlett-Packard, Palo Alto, CA) were used to present the visual stimuli and record responses.

### 2.3. Behavioral paradigm

We devised a behavioral task in which the processes for determining a behavioral goal were separated from those for specifying an action (Fig. 1A). During an inter-trial interval of ≥3 s, the participant was required to fixate on a fixation point that was presented at the center of the screen. After the inter-trial interval, an instruction message was presented at the center of the screen for 1 s. In the *visuo-goal* (*VG*) *condition*, a word indicating a goal ("Open" or "Close"), but not an action, was presented as an instruction message, which required the participant to take an appropriate action to open or close a door. However, in the *VG condition*, the participant did not decide which action to take at this point. In the *visuomotor* (*VM*) *condition*, the phrase "Tilt Right" or "Tilt Left" was used as an instruction message, which directly indicated the specific action to be taken. In the *control condition*, the phrase "Do Nothing" was used as an instruction message; the participant did not take any action in this condition. After a delay period (0.5–2.0 s), during which the participant was again required to fixate on the fixation point, a picture of an opened or closed sliding door was presented as a door cue (1.5 s). The participant had to tilt the joystick right or left corresponding to the combination of the instruction message and door cue (Fig. 1B). Specifically, in the *VG condition*, if the instruction message was "Open" and a closed door with the handle located at the leftmost or rightmost position was presented, the participant had to tilt the joystick right or left, respectively; and if the instruction message was "Close" and an opened door with the handle located at the rightmost or leftmost position was presented, the participant had to tilt the joystick right or left, respectively (*VG-go condition*). Conversely, if the instruction message was "Open" and any of the opened doors was presented (i.e., the door was already opened), the participant was not required to tilt the joystick; in the same manner, if the instruction message was "Close" and any of the closed doors was presented (i.e., the door was already closed), the participant was not required to tilt the joystick (*VG-no-go condition*). In the *VM condition*, if the instruction message was "Tilt Right" and a closed door with the handle located at the leftmost position or an opened door with the handle located at the rightmost position was presented, the participant had to tilt the joystick right; and if the instruction message was "Tilt Left" and a closed door with the handle located at the rightmost position or an opened door with the handle located at the leftmost position was presented, the participant had to tilt the joystick left (*VM-go condition*). Conversely, if the instruction message was "Tilt Right" and a closed door with the handle located at the rightmost position or an opened door with the handle located at the leftmost position was presented (i.e., the door could not move rightward), the participant was not required to tilt the joystick; in the same manner, if the instruction message was "Tilt Left" and a closed door with the handle located at the leftmost position or an opened door with the handle located at the rightmost position was presented (i.e., the door could not move leftward), the participant was not required to tilt the joystick (*VM-no-go condition*). In the *control condition*, the participant was not required to tilt the joystick whichever door cue was presented. After the surrounding of the door cue turned red (Go signal), the participant was required to execute the action within 1 s (*VG-go* and *VM-go conditions*) or do nothing (*VG-no-go*, *VM-no-go*, and *control conditions*). When the participant responded correctly, the message "Success" and a picture of an opened or closed door that corresponded to the participant's response were presented as feedback. If the participant did not respond correctly or tilted the joystick before Go signal onset, the message "Failure" and

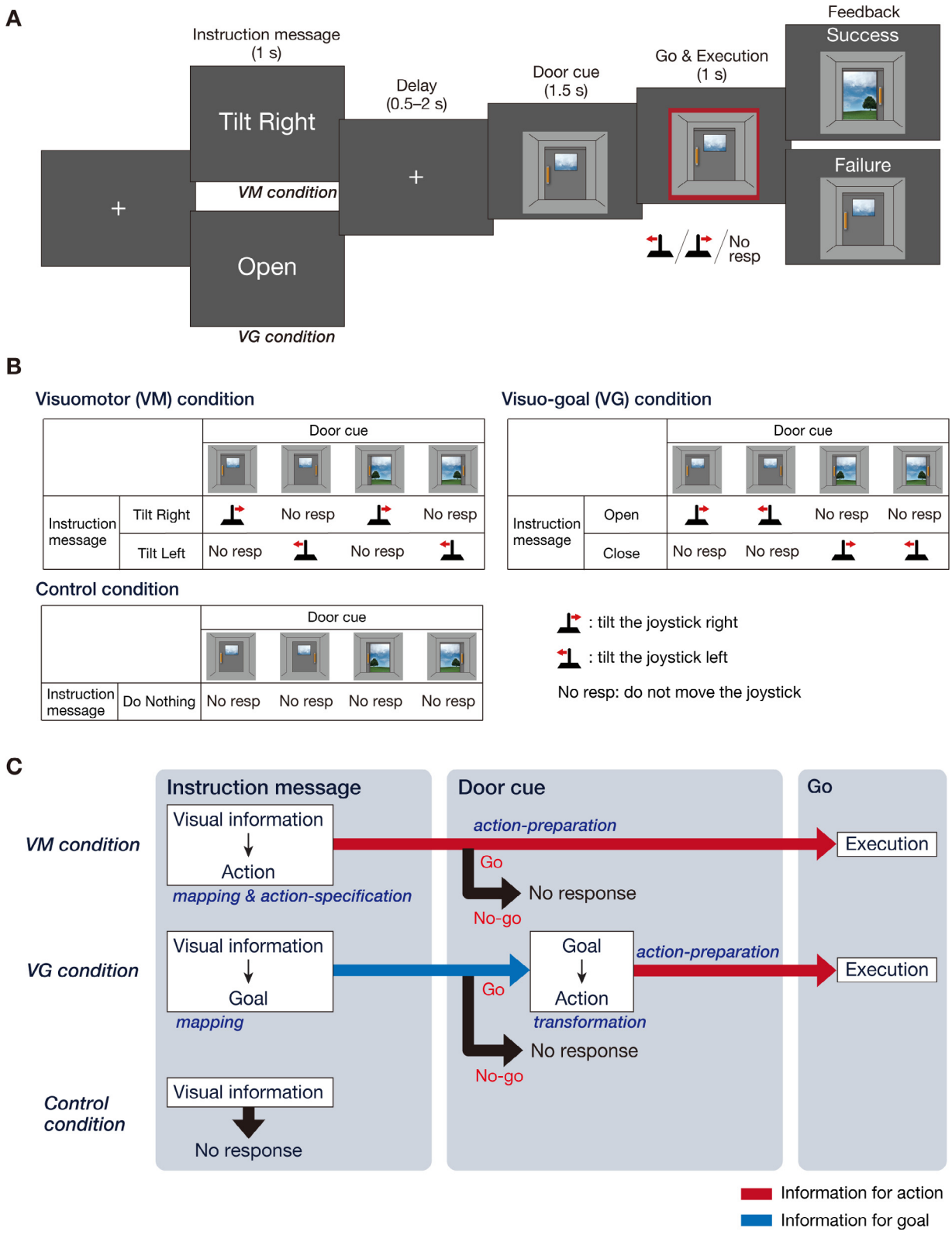


**Fig. 1.** The behavioral task, conditions, and schematic representation of the processing flow. (A) Temporal sequence of the behavioral task. After the inter-trial interval, a message was displayed (Instruction message) to instruct the participant to move the joystick leftward or rightward (*VM condition*, top), to open or close a door (*VG condition*, bottom), or to do nothing (*control condition*). A figure of a door appeared (Door cue) after the delay period. The participant was required to respond using the joystick immediately after the surrounding of the figure turned red (Go signal). (B) Combinations of instruction messages, door cues, and correct responses in each condition. (C) Schematic illustration of the *VM, VG*, and *control conditions*. In the *VM condition* (top), visual signals are mapped onto an action when the instruction message was presented, and then the participants specified an action. The participants have to retain the specified action until the door cue was presented, and then they have to prepare the action until the Go signal was presented (red arrow, *VM-go condition*). In the *VG condition* (middle), visual signals are mapped onto a behavioral goal when the instruction message was presented. The goal-related signals (blue arrow) are subsequently transformed into signals representing an action in accordance with the different door cues, and the participants have to prepare the action until the Go signal was presented (*VG-go condition*). In both conditions, some combinations of the instruction message and door cue indicate a no-go response (*VM-no-go* and *VG-no-go conditions*). In the *control condition*, the instruction message indicates no response. Thereafter, the participants do not have to perform any behavioral processing.

a picture of a door that corresponded to the participant's incorrect response were presented as feedback. The feedback was followed by an inter-trial interval of ≥3 s.

The behavioral task had the following characteristics. First, in the *VG condition*, an instruction message indicated that the participant should "open" or "close" the door, neither of which was associated with motor behavior such as tilting the joystick right or left. Thus, the participant could not select an action when the instruction message was presented. Second, in the *VM condition*, an instruction message indicated an action directly. At that point, the participant could specify an action such as tilting the joystick right or left. Third, each of the door cues was potentially associated with two kinds of motor behavior: (1) either tilting the joystick right or left and (2) doing nothing. In addition, the door cue was selected randomly from four different images. Therefore, the participant needed to maintain the information about the instruction message until the door cue was presented.

Before entering the MRI scanner, the participants performed a practice session that consisted of 20 trials to familiarize themselves with the task. The main experiment consisted of eight fMRI runs. Each run contained 40 trials (eight trials in each of the *VG-go, VG-no-go, VM-go, VM-no-go*, and *control conditions*). The order of conditions was pseudo-randomized and identical across all participants. The participants performed the task with their right hand in four runs, and they used their left hand in the remaining four runs. Fourteen participants used their right hand in the first four runs and their left hand in the remaining four runs, whereas the other 14 participants used their left hand in the first four runs and their right hand in the remaining four runs.

### 2.4. MRI scanning parameters

A 7.0 T scanner (Magnetom 7T; Siemens Healthcare, Erlangen, Germany) was used for the fMRI study. The participant's head was immobilized within a 32-channel receiver head coil and 1-channel transmitter head coil (NOVA). fMRI was performed using a multiband gradient- echo planar imaging (EPI) sequence (Moeller et al., 2010; repetition time [TR] = 1000 ms; echo time [TE] = 22.2 ms; field of view [FOV] = 208 × 208 $mm^2$; flip angle [FA] = 45º; matrix size = 130 × 130; 85 slices; slice thickness = 1.6 mm; GRAPPA = 2; multiband factor = 5; PPF = 7/8; BW = 1924 Hz/Px). To apply a field map distortion correction algorithm to the EPI images, multiband spin-echo EPIs with the opposite phase encoding directions were also scanned (TR = 3000 ms; TE = 60.4 ms; FOV = 208 × 208 $mm^2$; FA = 90º/180º; matrix size = 130 × 130; 85 slices; slice thickness = 1.6 mm; GRAPPA = 2; multiband factor = 5; PPF = 7/8; BW = 1924 Hz/Px). A 3.0 T scanner (Verio; Siemens Healthcare, Erlangen, Germany) with a 32-channel receiver head coil and 1-channel transmitter body coil was used for acquiring structural data to apply the Human Connectome Project (HCP) pipelines to the 7T-fMRI data. Two separate sets of whole-brain high-resolution T1-weighted (T1w) and T2-weighted (T2w) images were acquired using a 3D magnetization-prepared rapid-acquisition gradient-echo sequence (Mugler and Brookeman, 1990; TR = 2400 ms; TE = 2.24 ms; inversion time [TI] = 1060 ms; FOV = 256 × 240 $mm^2$; FA = 8º; matrix size = 320 × 300; 224 slices; slice thickness = 0.8 mm; GRAPPA = 2; BW = 210 Hz/Px) and a variable flip angle turbo spin-echo sequence (Mugler et al., 2000; TR = 3200 ms; TE = 560 ms; FOV = 256 × 240 $mm^2$; matrix size = 320 × 300; 224 slices; slice thickness = 0.8 mm; GRAPPA = 2; BW = 744 Hz/Px), respectively. To correct read-out distortion, spin-echo EPI field maps with the opposite phase encoding directions were also scanned (TR = 7700 ms; TE = 60 ms; FOV = 208 × 208 $mm^2$; FA = 78º/160º; matrix size = 104 × 104; 72 slices; slice thickness = 2 mm; PPF = 6/8; BW = 1850 Hz/Px).

### 2.5. fMRI data preprocessing

To investigate group-averaged task-related activity, we normalized the functional images from native space into standard space. To correct the distortion of the functional images measured by 7T-MRI, we adopted the minimal preprocessing pipelines (Glasser et al., 2013; Yamamoto et al., 2021) developed for the HCP (Glasser et al., 2016). We applied the HCP-style structural pipeline to the T1w and T2w images. First, image distortions resulting from gradient non-linearity were corrected. After the brain region was extracted, readout distortions were corrected using two spin-echo EPIs with opposite phase-encoding directions and the Topup toolbox (Andersson et al., 2003). Non-distorted T1w and T2w images were registered with cross-modal boundary-based registration (BBR; Greve and Fischl 2009). As the intensity of the T1w and T2w images still had biases, bias field correction was applied to the non-distorted images. Finally, we estimated the nonlinear registration matrix from native space to Montreal Neurological Institute (MNI) template space and applied this nonlinear registration to the T1w and T2w images.

The functional pipeline was also used to correct gradient non-linearity. To correct head motion, EPIs were registered into a single-band reference (SBRef) EPI, which was scanned at the beginning of each session, by estimating six parameters of rigid-body transformation from each EPI to SBRef EPI. In this study, we conducted structural and functional MRI sessions on different days. Thus, we calculated the session-specific field map from two SE-EPIs measured in the fMRI session. With this field map, we applied readout distortion correction to motion-corrected EPIs using the Topup toolbox. The transformation matrix from SBRef EPI to T1w images was estimated by BBR cross-modal registration method. Then, this BBR parameter was applied to non-distorted EPIs to register all EPIs into the T1w image. The resultant EPIs were transformed into MNI template space using the T1w-to-MNI parameters estimated in the structural pipelines. Finally, the image intensities of EPIs were normalized so that the average intensity of all images was 10,000. The normalized functional images were spatially smoothed using a Gaussian kernel of 4 mm full width at half maximum (FWHM) in the *x*, *y*, and *z* axes (Glasser et al., 2013).

### 2.6. fMRI data analysis

All statistical analyses were performed with the Statistical Parametric Mapping (SPM12) package (Wellcome Trust center for Neuroimaging, University College London, London, UK) and MATLAB 2021a (MathWorks, Natick, MA). A general linear model was fitted to the fMRI data for each participant (Friston et al., 1994; Worsley and Friston, 1995). Each run included 11 task-related regressors: instruction message in the *VM condition* (INST_VM), instruction message in the *VG condition* (INST_VG), instruction message in the *control condition* (INST_CON), door cue in the *VM-go condition* (DOOR_VM-go), door cue in the *VM-no-go condition* (DOOR_VM-no-go), door cue in the *VG-go condition* (DOOR_VG-go), door cue in the *VG-no-go condition* (DOOR_VG-no-go), door cue in the *control condition*, movement execution, success feedback, and failure feedback. These task-related regressors were modeled with stick functions and convolved with the canonical hemodynamic response function. Six motion parameters and their first derivatives were also included as nuisance regressors. The time series for each voxel was high-pass filtered at 1/128 Hz (Friston et al., 2002). For the advanced rapid sampling techniques used in this study, such as multi-band gradient-echo EPI, a first-order autoregressive model does not sufficiently capture the temporal correlations in time series data with higher sampling rates (Bollmann et al., 2018). Thus, the "FAST" model implemented in SPM12 was applied to address the temporal correlations in time series data with higher sampling rates (Corbin et al., 2018). Then, to calculate the estimated parameters, a least-squares estimation was performed on the high-pass filtered and pre-whitened data.

The parameter estimates for each regressor in each "contrast" image were submitted to second-level analysis (Holmes and Friston, 1998) with a flexible-factorial model. According to our hypotheses, we evaluated the following predefined contrasts. For counterbalancing effector-specific effects, all contrasts were calculated without distinguishing be-

tween the runs in which the participants used their right or left hand for the responses. First, we evaluated rule-based visuomotor mapping by subtracting the activity in the *control condition* from that in the *VM condition* during the presentation of the instruction cue: (INST_VM – INST_CON). Second, we evaluated rule-based visuo-goal mapping by subtracting the activity in the *control condition* from that in the *VG condition* during the presentation of the instruction cue: (INST_VG – INST_CON). Third, we evaluated action plan specification by subtracting the activity in the *VG condition* from that in the *VM condition* during the presentation of the instruction cue: (INST_VM – INST_VG). Fourth, we evaluated the transformation of a goal into an action by subtracting the difference in activity between the *VM-go* and *VM-no-go conditions* from the difference in activity between the *VG-go* and *VG-no-go conditions* during the presentation of the door cue: ([DOOR_VG-go – DOOR_VG-no-go] – [DOOR_VM-go – DOOR_VM-no-go]). Finally, we evaluated action preparation as the conjunction of the activity in the *VG-go condition* against the *VG-no-go condition* and that in the *VM-go condition* against the *VM-no-go condition* during the presentation of the door cue: ([DOOR_VG-go – DOOR_VG-no-go] & [DOOR_VM-go – DOOR_VM-no-go]). The resulting set of voxel values for each contrast constituted SPM{$t$}, which was transformed into normal distribution units (SPM{$z$}). The statistical threshold for the spatial extent test on the clusters, which was defined by the height threshold of $z = 3.09$, was set at $p < 0.05$ corrected for family-wise (Friston et al., 1996). We also tested for brain activity in the left and right rostral PMd as regions of interest (ROIs) after small volume correction (SVC) (Poldrack, 2007). We defined anatomical ROIs in the dorsal portion of the left and right rostral PMd using the Brainnetome Atlas (Fan et al., 2016). As the rostral PMd is located in the rostrodorsal part of the lateral Brodmann area 6, we used the left and right dorsolateral area 6 (A6dl) of the Brainnetome Atlas as ROIs for the analysis.

Brain regions were anatomically defined and labeled according to the co-planar stereotaxic atlas of the human brain (Mai et al., 2015). We used MRIcron (http://people.cas.sc.edu/rorden/mricron/index.html) to display the activation patterns on T1w MRI and volume-rendered images.

## 3. Results

### 3.1. Behavioral data

We excluded one participant's data because their proportion of correct responses was low (87.5%; see Materials and Methods and Table S1). The proportion of correct responses for the remaining 28 participants was > 90% (90.0–99.7%); therefore, we focused on brain activity during the trials in which the participants performed correctly. The reaction times (mean ± standard deviation) in the conditions accompanied by a movement were 434 ± 66 ms in the *VG-go condition* and 430 ± 64 ms in the *VM-go condition*. The reaction times did not differ between the *VG-go* and *VM-go conditions* (paired *t*-test; $t(27) = 0.89$, $p = 0.38$). Table S1 shows additional information about the proportion of correct responses and reaction times of each participant.

### 3.2. fMRI analyses

#### 3.2.1. Activation related to rule-based visuomotor and visuo-goal mapping

In the *VM condition*, the participants had to map an instruction message onto an action during the instruction period (Fig. 1A–C) because they then had to make a Go/No-go decision based on the mapped action plan. Therefore, we calculated activation related to rule-based visuomotor mapping, which was determined by subtracting the activity in the *control condition* from that in the *VM condition* during this period. This contrast was calculated without distinguishing between trials using the right or left hand (see Materials and Methods). This analysis revealed regions of significant activation in the bilateral PMd and left pre-supplementary motor area (pre-SMA) in the frontal lobe, and the left supramarginal gyrus (SMG) in the parietal lobe, as well as some parietal, temporal, and occipital areas such as the fusiform gyrus, inferior temporal gyrus, and inferior occipital gyrus ($p < 0.05$ corrected at the cluster level; Table 1 and Fig. 2A).

We next identified the brain regions that were activated in relation to mapping an instruction message onto a goal during the instruction period in the *VG condition* (Fig. 1A–C). We calculated activation related to rule-based visuo-goal mapping, which was determined by subtracting the activity in the *control condition* from that in the *VG condition* during the period from instruction message onset to the end of the delay period (instruction period, lasting 1.5–3.0 s; see Fig. 1A and C). These contrasts were also calculated without distinguishing trials using the right or left hand. The activated regions in the *VG condition* (Fig. 2B) were similar to those in the *VM condition* (Fig. 2A): this analysis revealed regions of significant activation in the bilateral PMd, left ventrolateral prefrontal cortex (vlPFC; Brodmann areas 9 and 44), left ventral premotor cortex (PMv), and left pre-SMA in the frontal lobe, and the left SMG and bilateral superior parietal lobule (SPL) in the parietal lobe, as well as some parietal, temporal, and occipital areas ($p < 0.05$ corrected at the cluster level; Table 2 and Fig. 2B).

#### 3.2.2. Activation related to action plan specification

We then examined activation related to action plan specification in visuomotor behavior. In the *VM condition*, once the participants mapped an instruction message onto an action based on a rule, they had to specify a plan for the action before the door cue was presented (Instruction message and Delay periods in Fig. 1A and C). By contrast, in the *VG condition*, the participants decided a plan for the goal, but could not specify an action in the same periods. To clarify the processes for specifying an action plan, we calculated the contrast of the processes by subtracting the activity in the *VG condition* from that in the *VM condition* during the instruction period (Fig. 1C). These contrasts were also calculated without distinguishing trials using the right or left hand. We found significant activation in the left PMd (Fig. 3), bilateral primary visual cortex (V1), bilateral visual areas V2 and V3, and bilateral fusiform gyrus ($p < 0.05$ corrected at the cluster level; Table 3). The activation area of the left PMd was located more caudal to that related to rule-based visuomotor mapping or visuo-goal mapping (Fig. 2 and Tables 1 and 2).

#### 3.2.3. Activation related to the transformation of a goal into an action

We next identified the regions related to the transformation of a goal into an action in visuo-goal behavior. We investigated activation in response to the door cue (Door cue period in Fig. 1A), when the participants could decide an action based on the goal in the *VG-go condition*. In the *control condition*, the participants did not have to attend to a door cue because they were not required to tilt the joystick whichever door cue was presented. Therefore, we subtracted the activation in the *go* conditions (*VM-go* and *VG-go conditions*) from than in the *no-go* conditions (*VM-no-go* and *VG-no-go conditions*).

We first determined activation related to the transformation of a goal into an action by subtracting the activity of the *VM conditions* from that of the *VG conditions* (i.e., [*VG-go – VG-no-go*] – [*VM-go – VM-no-go*]) during the presentation of the door cue (Door cue period, lasting 1.5 s). As with the calculation of activation for the instruction message, these contrasts were also calculated without distinguishing trials using the right or left hand. We found no significant activation when whole brain analysis was performed ($p < 0.05$ corrected at the cluster level), but we found 17 significant voxels in a cluster within the left rostral PMd when we applied a height threshold of $p < 0.001$ (uncorrected). We then performed SVC analysis for the region of the left rostral PMd (blue outlined area in Fig. 4) defined using the Brainnetome Atlas (Fan et al., 2016; see Materials and Methods). In this analysis, we focused on the rostral portion of the PMd as the ROI for the following two reasons. First, our previous findings in monkeys demonstrated that when subjects selected an action based on a goal, neurons in the rostral PMd represented an action more often than neurons in the caudal PMd or primary motor cortex (M1)

**Table 1**
Instruction message-related activation related to rule-based visuomotor mapping.

| Spatial extent test | | MNI coordinates (mm) | | | | | |
|---|---|---|---|---|---|---|---|
| Cluster size ($mm^3$) | $P_{FWE-corr}$ | x | y | z | *z* value | Hem | Anatomical region |
| *VM – control* | | | | | | | |
| 4608 | $6.84 \times 10^{-13}$ | −38 | −76 | −11 | 7.37 | L | Fusiform gyrus, posterior part |
| | | −32 | −64 | −14 | 5.53 | L | Fusiform gyrus |
| 2630 | $1.35 \times 10^{-8}$ | −27 | −6 | 51 | 6.84 | L | Middle frontal gyrus |
| | | −30 | −12 | 66 | 4.43 | L | Superior frontal gyrus, lateral part |
| 1499 | $1.24 \times 10^{-5}$ | −6 | 5 | 56 | 6.23 | L | Superior frontal gyrus, medial part |
| | | −8 | 10 | 45 | 3.22 | L | Cingulate gyrus |
| 938 | $6.93 \times 10^{-4}$ | 37 | −52 | −19 | 5.63 | R | Fusiform gyrus |
| | | 44 | −60 | −18 | 4.81 | R | Inferior temporal gyrus |
| 2875 | $3.55 \times 10^{-9}$ | 28 | −76 | −10 | 5.55 | R | Fusiform gyrus |
| | | 31 | −84 | −13 | 4.93 | R | Fusiform gyrus, posterior part |
| | | 39 | −83 | −10 | 4.79 | R | Inferior occipital gyrus |
| 3027 | $1.58 \times 10^{-9}$ | 31 | −4 | 56 | 5.51 | R | Middle frontal gyrus |
| | | 23 | −4 | 46 | 4.59 | R | Superior frontal gyrus, lateral part |
| 1278 | $5.62 \times 10^{-5}$ | −44 | −36 | 40 | 5.02 | L | Supramarginal gyrus |
| 836 | $1.56 \times 10^{-3}$ | −25 | −89 | 13 | 4.06 | L | Medial occipital gyrus |

Statistical threshold was family-wise-corrected (FWE-corr) ($p < 0.05$) at the cluster level with a height threshold of $z > 3.09$. Hem, hemisphere; L, left; MNI, Montreal Neurological Institute; R, right; VM, visuomotor.

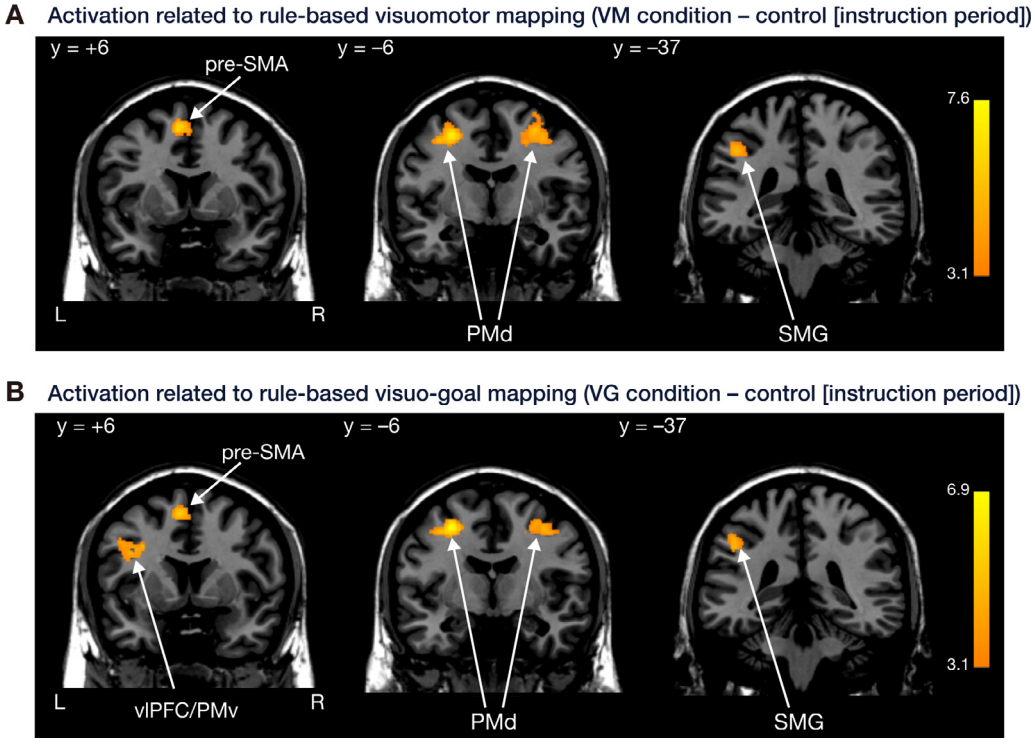


**Fig. 2.** Functional magnetic resonance imaging results for instruction message-related activation. (A) Activation related to rule-based visuomotor mapping determined by the contrast of the *visuomotor* (*VM*) *condition* against the *control condition* during the instruction period. Statistical maps show significant activation in a parieto-frontal network including the bilateral dorsal premotor cortex (PMd), left pre-supplementary motor area (pre-SMA), and left supramarginal gyrus (SMG), as well as the bilateral fusiform gyrus (FFG) (see Table 1). (B) Activation related to rule-based visuo-goal mapping determined by contrast of the *visuo-goal* (*VG*) *condition* against the *control condition* during the instruction period. Statistical maps show significant activation in the bilateral PMd, left ventrolateral prefrontal cortex (vlPFC)/ventral premotor cortex (PMv), left pre-SMA, left SMG, as well as the bilateral superior parietal lobule (SPL) and right posterior angular gyrus (see Table 2). Color bar indicates *t*-values. Numbers indicate the Montreal Neurological Institute (MNI) coordinates (in mm) in the coronal direction. For both panels, $p < 0.05$ corrected at the cluster level, with height threshold $z > 3.09$. L, left; R, right.

(Nakayama et al., 2016, 2008). Second, Badre et al. (2010) showed that the left rostral PMd in humans is critical for learning abstract behavioral rules, but the caudal PMd is not. By performing this analysis, we found one significant voxel within the ROI of the left rostral PMd (voxel level $p < 0.05$, SVC with family-wise correction; within the blue outlined area in Fig. 4 and Table 4). We then applied the same SVC analysis to the right rostral PMd, which was also defined using the Brainnetome Atlas, and found no significant voxels within the ROI. These results indicate that although the activated area is small, only the left rostral PMd appears to be involved in transforming a goal into an action.

### 3.2.4. Activation related to action preparation

We then tested activation related to preparation for a planned action, which is a common process in visuomotor and visuo-goal behavior. The action preparation process was determined by the conjunction of the activity of the *VG conditions* (*VG-go – VG-no-go*) and that of the

**Table 2**
Instruction message-related activation related to rule-based visuo-goal mapping.

| Spatial extent test | | MNI coordinates (mm) | | | | | |
|---|---|---|---|---|---|---|---|
| Cluster size ($mm^3$) | $P_{FWE-corr}$ | x | y | z | *z* value | Hem | Anatomical region |
| *VG – control* | | | | | | | |
| 2306 | $8.42 \times 10^{-8}$ | −28 | −6 | 50 | 6.75 | L | Middle frontal gyrus |
| 1585 | $7.00 \times 10^{-6}$ | −6 | 7 | 56 | 5.53 | L | Superior frontal gyrus, medial part |
| 2322 | $7.66 \times 10^{-8}$ | 39 | −4 | 48 | 5.40 | R | Precentral gyrus |
| | | 47 | −1 | 50 | 5.06 | R | Middle frontal gyrus |
| 1483 | $1.38 \times 10^{-5}$ | −32 | 4 | 34 | 4.81 | L | Inferior frontal gyrus, opercular part |
| | | −48 | −1 | 35 | 4.23 | L | Precentral gyrus |
| 500 | $2.94 \times 10^{-2}$ | 42 | −54 | −6 | 4.74 | R | Inferior temporal gyrus |
| 1184 | $1.10 \times 10^{-4}$ | −46 | −38 | 40 | 4.74 | L | Supramarginal gyrus |
| 770 | $2.68 \times 10^{-3}$ | −28 | −57 | 51 | 4.54 | L | Superior parietal lobule |
| 573 | $1.48 \times 10^{-2}$ | 31 | −51 | 53 | 4.49 | R | Superior parietal lobule |
| 1212 | $8.94 \times 10^{-5}$ | 32 | −81 | 34 | 4.34 | R | Posterior angular gyrus |
| | | 26 | −75 | 45 | 4.12 | R | Arcus parieto-occipitalis, ant. division / Posterior angular gyrus |
| 872 | $1.16 \times 10^{-3}$ | −24 | −72 | 32 | 4.09 | L | Arcus parieto-occipitalis, ant. division |
| | | −20 | −68 | 45 | 3.77 | L | Superior parietal lobule |
| 590 | $1.27 \times 10^{-2}$ | 28 | −88 | 11 | 4.02 | R | Medial occipital gyrus |

Statistical threshold was family-wise-corrected (FWE-corr) ($p < 0.05$) at the cluster level with a height threshold of $z > 3.09$. Hem, hemisphere; L, left; MNI, Montreal Neurological Institute; R, right; VM, visuomotor.

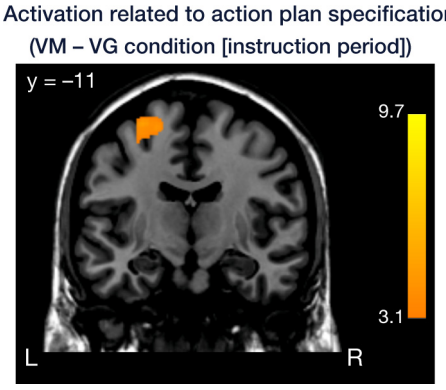


**Fig. 3.** Functional magnetic resonance imaging results for activation related to action plan specification determined by activation in the *visuomotor* (*VM*) *condition* against that in the *visuo-goal* (*VG*) *condition* during the instruction period. Statistical maps show significant activation in the left dorsal premotor cortex (PMd), as well as some occipital and parietal regions (see Table 3). Color bar indicates *t*-values. The number indicates the MNI coordinate (in mm) in the coronal direction. For both panels, $p < 0.05$ corrected at the cluster level, with height threshold $z > 3.09$. L, left; R, right.

*VM conditions* (*VM-go – VM-no-go*) during the Door cue period. These contrasts were also calculated without distinguishing trials using the right or left hand. The analysis revealed regions of significant activation in the bilateral PMd extending to the bilateral M1 and left primary somatosensory cortex (S1), bilateral pre-SMA/SMA, bilateral putamen, and bilateral thalamic nuclei (Fig. 5), as well as some occipital areas ($p < 0.05$ corrected at the cluster level; Table 5).

### 3.3. Spatial distribution of activation in the PMd

We found activation of the PMd in five contrasts related to rule-based visuomotor (Fig. 2A) and visuo-goal (Fig. 2B) mapping, action plan specification (Fig. 3A), transformation of a goal into an action (Fig. 4), and action preparation (Fig. 5). We also found activation of the right PMd in three contrasts related to rule-based visuomotor (Fig. 2A) and visuo-goal (Fig. 2B) mapping and action preparation (Fig. 5). These activation areas were generally separate from each other, but there was some overlap. Fig. 6 shows the activated voxels in each contrast on the lateral surface of the left and right hemispheres in terms of visuomotor behavior (Fig. 6A) and visuo-goal behavior (Fig. 6B). The activated areas related to rule-based visuomotor mapping (magenta in Fig. 6A) overlapped with those related to rule-based visuo-goal mapping (blue in Fig. 6B) in many regions of the PMd (light purple in Fig. 6C) in each hemisphere, although the former extended more caudally and medially than the latter. The activated areas related to action plan specification (yellow) were located more caudally and dorsally than those related to rule-based visuomotor (magenta) and visuo-goal (blue) mapping in the left PMd. The activated areas related to action plan specification partly overlapped with those related to rule-based visuomotor mapping (light red in Fig. 6A and C), but did not overlap with those related to rule-based visuo-goal mapping (Fig. 6C). The three areas were located in the rostral and ventral portion of the caudal sector of the PMd, or simply the PMd. In contrast, the activated area related to the transformation of a goal into an action (green) was located in the rostral sector of the PMd, or the pre-PMd (Abe and Hanakawa, 2009; Picard and Strick, 2001), in the left hemisphere. The activated areas related to action preparation (red) were located at the most caudal portion of the bilateral PMd, and they extended rostrally to the areas where rule-based visuomotor and visuo-goal mapping were observed and caudally to the M1 in both hemispheres and the left S1. The activated areas of rule-based visuomotor mapping and those of rule-based visuo-goal mapping mostly overlapped with each other in both hemispheres (light purple in Fig. 6C). These results suggest that the PMd is parcellated in terms of achieving goal-directed motor behavior in humans and these parcellations overlap in part with each other spatially and functionally.

## 4. Discussion

In the present study, we examined the neural representation related to step-by-step planning processes for visuomotor and visuo-goal behavior in humans using fMRI. For visuomotor behavior, we examined three steps of the planning process. First, during the process for rule-based visuomotor mapping, we found activation of the ventrorostral portion of the bilateral PMd, as well as the SMG in the parietal cortex. Second, during the process for action plan specification, we found activation of the dorsocaudal portion of the left PMd. Finally, during the process for action preparation, we found activation of the caudal portion of the bilateral PMd and the activation areas extended rostrally to the ventrorostral portion of the PMd and caudally to the M1 and S1. Conversely, for visuo-goal behavior, we examined another three steps of the planning process. First, during the process for rule-based visuo-goal mapping, we found activation of the ventrorostral portion of the bilateral PMd, as well as the SMG and SPL. Second, during the process for the transfor-

**Table 3**
Instruction message-related activation related to action plan specification.

| Spatial extent test | | MNI coordinates (mm) | | | | | |
|---|---|---|---|---|---|---|---|
| Cluster size ($mm^3$) | $P_{FWE\text{-}corr}$ | x | y | z | *z* value | Hem | Anatomical region |
| *VM – VG* | | | | | | | |
| 5890 | $2.44 \times 10^{-15}$ | −16 | −91 | −10 | Inf. | L | Striate area / Inferior lingual gyrus, medial part |
| | | −27 | −83 | −13 | Inf. | L | Fusiform gyrus / Inferior lingual gyrus, medial part |
| | | −38 | −78 | −10 | 7.55 | L | Fusiform gyrus, posterior part |
| 4887 | $1.93 \times 10^{-13}$ | 18 | −88 | −6 | Inf. | R | Inferior lingual gyrus, medial part |
| | | 28 | −76 | −8 | 7.52 | R | Fusiform gyrus |
| 1290 | $5.15 \times 10^{-5}$ | −28 | −11 | 66 | 4.67 | L | Superior frontal gyrus, lateral part |
| | | −28 | −14 | 58 | 4.51 | L | Precentral gyrus |

Statistical threshold was family-wise corrected (FWE-corr) ($p < 0.05$) at the cluster level with a height threshold of $z > 3.09$. Hem, hemisphere; Inf., infinity; L, left; MNI, Montreal Neurological Institute; R, right; VG, visuo-goal; VM, visuomotor.

**Table 4**
Door cue-related activation related to the transformation of a goal into an action.

| | MNI coordinates (mm) | | | | | |
|---|---|---|---|---|---|---|
| Number of voxels | x | y | z | *z* value | Hem | Anatomical region |
| *(VG-go – VG-no-go) – (VM-go – VM-no-go)* | | | | | | |
| 1 | −12 | 5 | 64 | 3.75 | L | Superior frontal gyrus, lateral part |

Statistical threshold was family-wise corrected ($p < 0.05$) at the voxel level with small volume correction within the region of interest of the left rostral dorsal premotor cortex. Hem, hemisphere; L, left; MNI, Montreal Neurological Institute; VG, visuo-goal; VM, visuomotor.

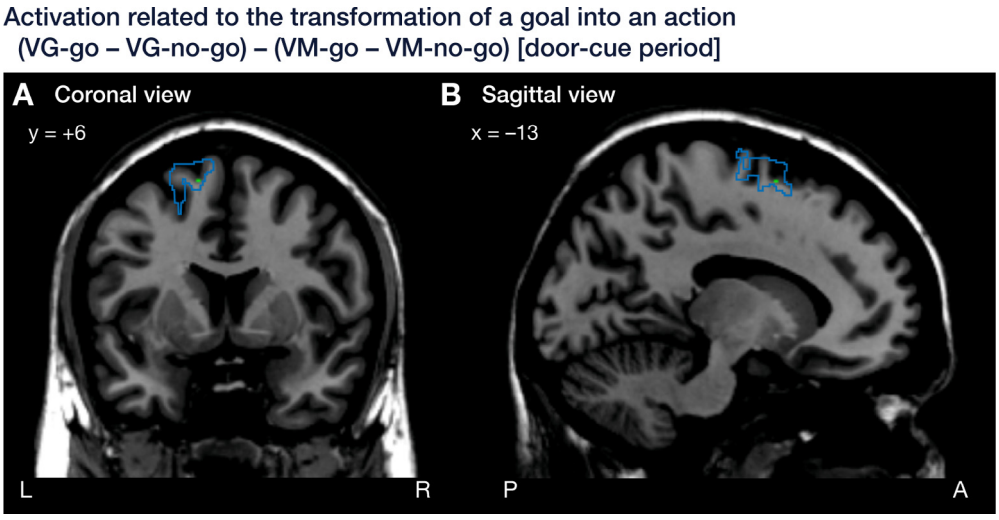


**Fig. 4.** Functional magnetic resonance imaging results for activation related to the transformation of a goal into an action. The contrast was determined by subtraction of the activity for the *visuomotor* (*VM*)*-go condition* against the *VM-no-go condition* from that for the *visuo-goal* (*VG*) *condition* against the *VG-no-go condition* (i.e., [*VG-go – VG-no-go*] – [*VM-go – VM-no-go*]) during the door cue period. A significant voxel ($p < 0.05$ with family-wise, small volume correction) in the left dorsal premotor cortex (PMd) was observed, and is shown in green in coronal (A) and sagittal slices (B). The blue outlines show the area of the left dorsolateral area 6 (A6dl) of the Brainnetome Atlas (Fan et al., 2016). Numbers indicate the MNI coordinates (in mm) in the coronal (A) and sagittal (B) direction. A, anterior; L, left; P, posterior; R, right.

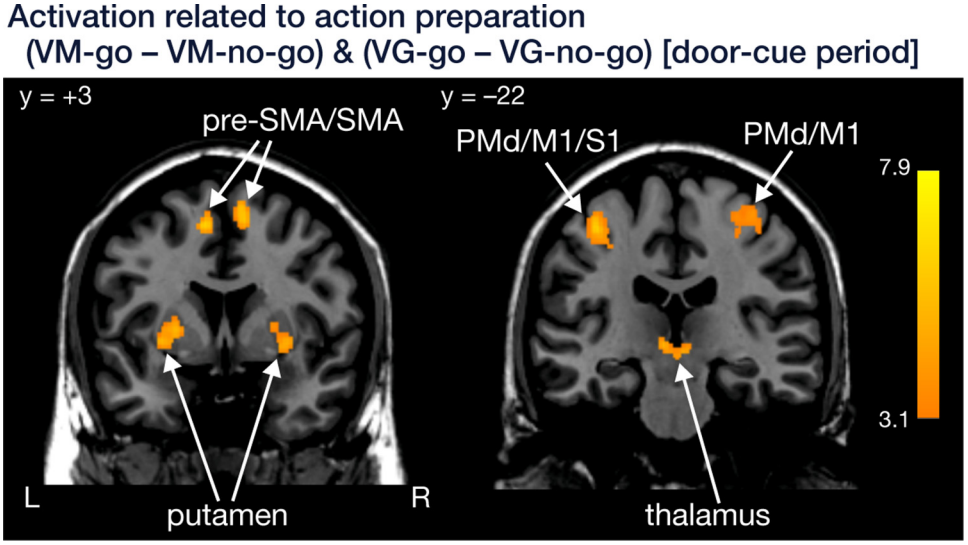


**Fig. 5.** Functional magnetic resonance imaging results for activation related to action preparation determined by the conjunction of activity for the *visuomotor* (*VM*) *conditions* (*VM-go – VM-no-go*) and that for the *visuo-goal* (*VG*) *conditions* (*VG-go – VG-no-go*) during the door cue period. Statistical maps show significant activation in the bilateral dorsal premotor cortex (PMd), bilateral primary motor cortex (M1), left primary somatosensory cortex (S1), bilateral pre-supplementary motor area (pre-SMA) and supplementary motor area (SMA), bilateral putamen, and bilateral thalamic nuclei, as well as some occipital regions (see Table 5). Numbers indicate the MNI coordinates (in mm) in the coronal direction. Color bar indicates *t*-values. For the panel, $p < 0.05$ corrected at the cluster level, with height threshold $z > 3.09$. L, left; R, right.

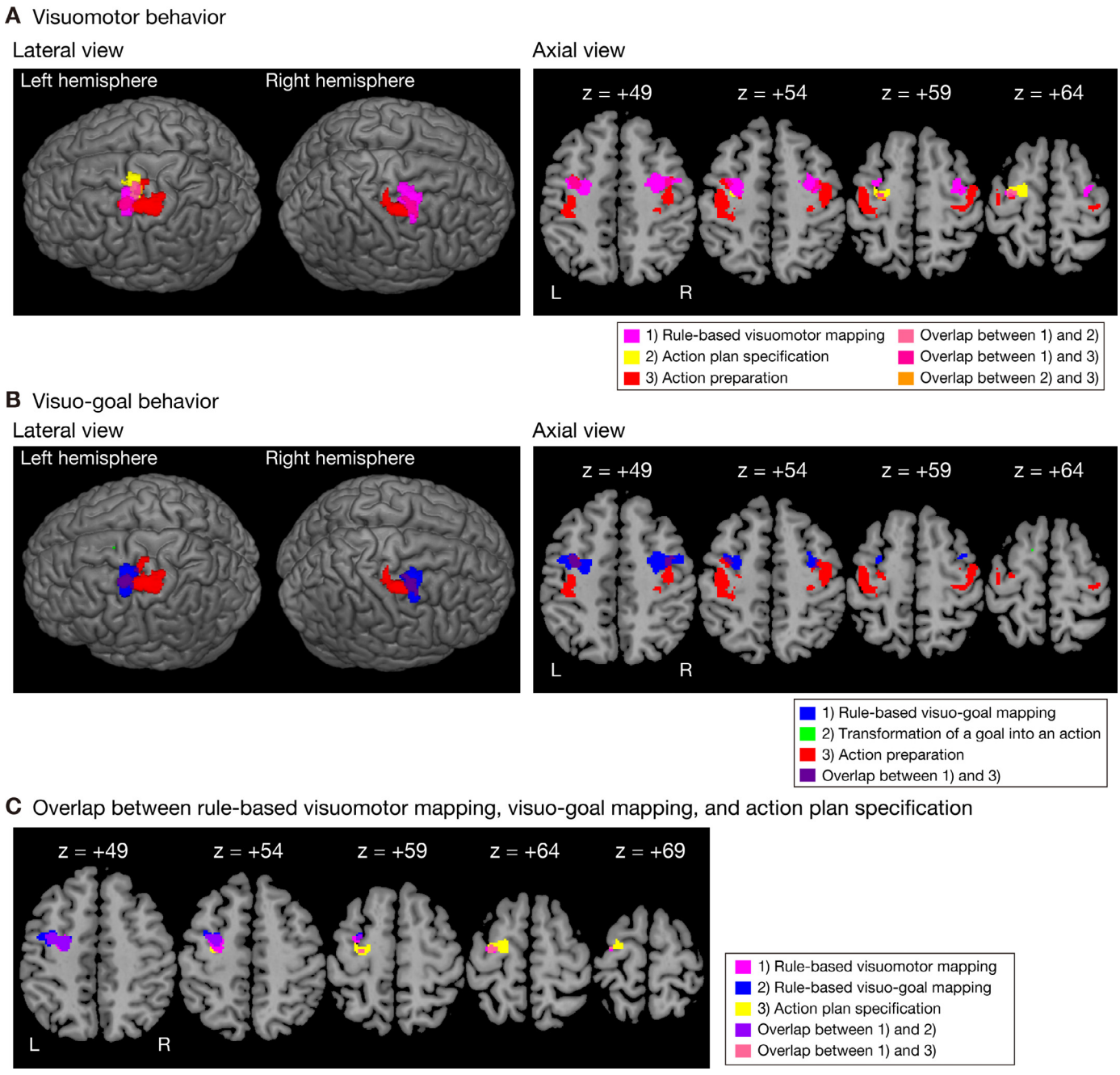


**Fig. 6.** Spatial distributions of functional magnetic resonance imaging (fMRI) activity within the dorsal premotor cortex (PMd) in different conditions or task phases. (A) Activated areas of the PMd in terms of visuomotor behavior. Activated areas related to rule-based visuomotor mapping (magenta, results from Fig. 2A), action plan specification (yellow, results from Fig. 3A), and action preparation (red, results from Fig. 5) were superimposed on lateral (left) and axial (right) views of the brain in both hemispheres. The activated areas related to action preparation (red) extend to the bilateral primary motor cortex (M1) and left primary somatosensory cortex (S1). Light red areas indicate voxels related to rule-based visuomotor mapping and action plan specification, hot pink areas indicate voxels related to rule-based visuomotor mapping and action preparation, and orange areas indicate voxels related to action plan specification and action preparation. (B) Activated areas of the PMd in terms of visuo-goal behavior. Activated areas related to rule-based visuo-goal mapping (blue, results from Fig. 2B), transformation of a goal into an action (green, results from Fig. 4), and action preparation (red, results from Fig. 5) were superimposed on lateral (left) and axial (right) views of the brain in both hemispheres. Purple areas indicate voxels related to rule-based visuo-goal mapping and action preparation. (*C*) Activated area of the PMd related to rule-based visuomotor mapping, visuo-goal mapping, and action plan specification. Activated areas related to rule-based visuomotor mapping (magenta), rule-based visuo-goal mapping (blue), and action plan specification (yellow) were superimposed on axial views of the brain in both hemispheres. Light purple areas indicate voxels related to rule-based visuomotor mapping and rule-based visuo-goal mapping, and light red areas indicate voxels related to rule-based visuomotor mapping and action plan specification. Numbers indicate the MNI coordinates (in mm) in the axial direction. L, left; R, right.

**Table 5**
Door cue-related activation related to action preparation.

| Spatial extent test | | MNI coordinates (mm) | | | | | |
|---|---|---|---|---|---|---|---|
| Cluster size ($mm^3$) | $P_{FWE-corr}$ | x | y | z | *z* value | Hem | Anatomical region |
| *(VM-go – VM-no-go) & (VG-go – VG-no-go)* | | | | | | | |
| 2867 | $3.71 \times 10^{-9}$ | −38 | −14 | 54 | 7.63 | L | Precentral gyrus |
| | | −30 | −32 | 56 | 3.77 | L | Postcentral gyrus |
| 2621 | $1.42 \times 10^{-8}$ | 40 | −11 | 54 | 7.35 | R | Precentral gyrus |
| 1323 | $4.10 \times 10^{-5}$ | −9 | 5 | 54 | 6.34 | L | Superior frontal gyrus, medial part |
| | | −8 | −9 | 58 | 5.45 | L | Paracentral lobule |
| 1130 | $1.62 \times 10^{-4}$ | 7 | −1 | 59 | 5.90 | R | Superior frontal gyrus, medial part |
| 1413 | $2.21 \times 10^{-5}$ | −30 | 2 | −2 | 5.49 | L | Putamen |
| 872 | $1.16 \times 10^{-3}$ | −6 | −20 | −2 | 5.48 | L | Thalamus |
| | | 2 | −20 | −6 | 4.80 | R | Midbrain |
| | | −4 | −32 | −8 | 4.28 | L | Brachium of the inferior colliculus |
| 762 | $2.86 \times 10^{-3}$ | −33 | −3 | 48 | 5.30 | L | Middle frontal gyrus |
| 856 | $1.32 \times 10^{-3}$ | 29 | 2 | −3 | 4.95 | R | Putamen |
| 451 | $4.71 \times 10^{-2}$ | −27 | −14 | 61 | 4.20 | L | Superior frontal gyrus, lateral part |
| | | −27 | −17 | 70 | 3.65 | L | Precentral gyrus |

Statistical threshold was family-wise corrected (FWE-corr) ($p < 0.05$) at the cluster level with a height threshold of $z > 3.09$. Hem, hemisphere; L, left; MNI, Montreal Neurological Institute; R, right; VG, visuo-goal; VM, visuomotor.

mation of a goal into an action, we found activation of the rostral portion of the left PMd. Finally, during the process for action preparation, which is shared with visuomotor behavior, we found activation of the caudal portion of the bilateral PMd as well as the ventrorostral portion of the PMd, M1, and S1. Thus, the PMd was activated throughout all of the planning processes of visuomotor and visuo-goal behavior. The activated areas in each of the left and right PMd were spatially segregated, but overlapped partially. These findings indicate that there are subregions in the bilateral PMd and these subregions make a functional gradient for achieving goal-directed behavior.

### 4.1. A step-by-step planning process for visuomotor behavior

In visuomotor behavior, we first map a visual stimulus onto an action in a rule-based manner. We found activation of the ventrorostral portion of the bilateral PMd during the process for rule-based visuomotor mapping (Fig. 2A). The location of activation is considered to be reasonable because the ventrorostral part of the PMd of monkeys receives inputs from the vlPFC via the dorsolateral or dorsomedial prefrontal cortex (Takahara et al., 2012). Previously, we found that neurons in the vlPFC of monkeys encode visual object signals, but those in the PMd do not (Nakayama et al., 2016; Yamagata et al., 2012). In the present study, the participants had to recognize a written phrase before mapping it to an action or a goal. Therefore, the ventrorostral portion of the PMd is thought to be involved in rule-based visuomotor mapping in cooperation with the vlPFC, and may be a gateway within the PMd for visually guided goal-directed behavior.

After the mapping process in the *VM condition*, the participants had to specify an action plan during an instruction period that was maintained until the door cue was presented, when the participants could (*VM-go condition*) or could not (*VM-no-go condition*) decide to take the action. We found activation related to action plan specification in the dorsocaudal portion of the left PMd. Although some activation areas overlapped, the activation area related to action plan specification in the PMd (yellow in Fig. 6A and C) was located more caudally to that of rule-based visuomotor mapping (magenta). As the process for action plan specification is thought to be more concrete than that for rule-based visuomotor mapping and the two activation areas overlapped partially, the results indicate that more abstract planning processes were represented in the more rostral portion of the PMd. These two areas constitute a part of a rostrocaudal functional gradient from abstract to concrete planning processes, as discussed later.

Once the participants made the “go” decision, they had to prepare the planned action. We found activation related to action preparation in the caudal portion of the bilateral PMd (Fig. 5). The activated region was located more caudally than the regions related to rule-based visuomotor mapping and action specification. In addition, it expanded caudally to the M1 in both hemispheres (red in Fig. 6A) as well as rostrally to the ventrorostral portion of the PMd. The activated location was plausible because the caudal portion of the PMd is adjacent to the M1, which is a cortical center for executing actions (Evarts, 1964; Kalaska, 2009), and the M1 is also involved in action preparation (Nakayama et al., 2016; Tanji and Evarts, 1976). Additionally, we found activation in the bilateral putamen, which is considered to be involved in action preparation (Alexander and Crutcher, 1990; Apicella et al., 1992) and connects to the PMd (Alexander et al., 1986; Takada et al., 1998). These observations suggest that the caudal portion of the PMd is hierarchically closer to the output stage within the PMd.

Taken together, also in terms of achieving visuomotor behavior, these results support the hypothesis that there is a functional gradient within the PMd: the more rostral region processes abstract planning, while the more caudal region processes more concrete information (Abe and Hanakawa, 2009; Badre and D’Esposito, 2009; Badre and Nee, 2018; Cisek and Kalaska, 2005; Nakayama et al., 2016, 2008; Picard and Strick, 2001).

### 4.2. A step-by-step planning process for visuo-goal behavior

In visuo-goal behavior, we first map a visual stimulus onto a goal in a rule-based manner. We found activation of the bilateral ventrorostral portion of the PMd during the process for rule-based visuo-goal mapping (Fig. 2B). This is consistent with our previous findings in monkeys that show neurons in the ventrorostral PMd encode goals (Nakayama et al., 2016, 2008; Yamagata et al., 2012). The location of the activation area was similar to that of rule-based visuomotor mapping (Fig. 6C), suggesting that the ventrorostral portion of the PMd is also involved in rule-based visuo-goal mapping in cooperation with the vlPFC.

The neural representation of a goal plan is then transformed into that of an action plan at a certain point. In the present study, after a door cue was presented, the participants had to decide a specific action based on the goal plan (Fig. 1C). We found a significantly activated small region in the rostral PMd in the left hemisphere, which represented the process for the transformation of a goal into an action (Fig. 4). As shown in Fig. 6B (green), the activation region was rostral to the other activation area within the left PMd. In addition, no significant voxels were found in the ROI in the right hemisphere. Taken together, the present results indicate that although the activation area is restricted, the left PMd may be involved in transforming a goal into an action. In addition,

the activated region was located in the rostral portion of the left PMd and away from the other activated regions (Fig. 6B and C), suggesting the existence of a unique portion of the left PMd that is involved in transforming a goal into an action.

As with visuomotor behavior, once the action is transformed and the participants make a "go" decision, they have to prepare the planned action. As mentioned in the previous section, we found activation related to action preparation in the caudal portion of the bilateral PMd (Fig. 5). The activated region was located just caudal to the regions related to rule-based visuo-goal mapping with some overlap (red in Fig. 6B).

These findings suggest that there also exists a functional gradient within the PMd in terms of the processes for mapping a visual stimulus onto a goal and preparing an action, but the transformation process may be independent from this gradient.

### 4.3. Neural substrate of rule-based visuomotor and visuo-goal mapping

As mentioned earlier, we found activation in the ventrorostral portion of the PMd in relation to rule-based visuomotor and visuo-goal mapping, and these two types of activation overlapped in the left and right hemispheres (magenta and blue in Fig. 6). These results can be interpreted by the following two points. First, in visuomotor and visuo-goal behavior, we have to map a visual signal onto a behavioral component. One interpretation is that the ventrorostral PMd plays a role in the mapping process, irrespective of visuomotor or visuo-goal behavior. Second, rule-based visuomotor behavior may contain a component of visuo-goal mapping, because it is considered that visuomotor behavior does not distinguish a goal from an action. In other words, visuomotor behavior is regarded as a special case of visuo-goal behavior in that a goal and an action can be fixed simultaneously in accordance with a visual signal. Therefore, the ventrorostral PMd may be involved in the process for mapping a visual signal onto a goal, but not an action. In either case, the present results indicate that rule-based visuomotor and visuo-goal mapping share the same neural substrates. However, it remains elusive whether the same neurons in the ventrorostral PMd are involved in rule-based visuomotor mapping and rule-based visuo-goal mapping. Further studies are needed to compare cell activity for visuomotor behavior with that for visuo-goal behavior.

We also found activation of the left SMG in the parietal cortex for the process of rule-based visuomotor and visuo-goal mapping (Fig. 2). It is reasonable that the SMG is active during the instruction period for the following reasons. First, both are involved in semantic processing (Chou et al., 2006; Sakai, 2005; Stoeckel et al., 2009) and verbal working memory (Deschamps et al., 2014; Koelsch et al., 2009; Salmon et al., 1996). As we instructed the participants which action (*VM condition*) or goal (*VG condition*) to take by using written phrases, the activation of the SMG may represent the processes of semantic understanding of the instruction message and storage of the information of the instruction message at a verbal level. Second, a left SMG lesion in humans causes ideomotor apraxia, which is a cognitive disorder characterized by the inability to perform accurate movements on verbal command, even though the patient understands the meaning of the command and does not have aphasia or paralysis (Alexander et al., 1992; Heilman et al., 1982). One interpretation is that ideomotor apraxia is caused by deficits in creating conceptual knowledge for an action (Buxbaum and Randerath, 2018; Kemmerer et al., 2012; Tranel et al., 2003), such as a behavioral goal in the present study. Finally, diffusion tensor imaging studies indicate that the SMG is structurally connected to the lPFC and PMv (Kamali et al., 2014; Martino et al., 2013; Rushworth et al., 2006; Uddin et al., 2010; Wang et al., 2016), which we previously found to be involved in determining a goal in monkeys (Nakayama et al., 2016, 2008; Yamagata et al., 2012, 2009), and we found activation for rule-based visuo-goal mapping in humans in the present study. Considering that the SMG was not activated in the other contrasts (Figs. 3–5), the present results indicate that they are involved in the processes for mapping visual signals onto an action and a goal in goal-directed motor behavior.

### 4.4. Subregions of the PMd related to the step-by-step planning processes in visuomotor and visuo-goal behavior

In our previous studies, we showed the presence of a rostrocaudal functional gradient within the PMd in monkeys for planning processes of visuo-goal behavior (Nakayama et al., 2016, 2008). Indeed, in the present study, the activated areas in each process were generally separated, but overlapped partially with each other, implying the existence of a functional gradient also in the human PMd. Overall, cognitive processes (rule-based visuomotor and visuo-goal mapping and transformation of a goal into an action) were represented in two rostral parts of the PMd (ventrorostral and rostral subregions), whereas action-related processes (action plan specification and action preparation) were represented in two caudal parts (dorsocaudal and caudal subregions). Specifically, we classified activation of the PMd into four subregions: (1) activation related to rule-based visuomotor mapping (magenta in Fig. 6) and visuo-goal mapping (cyan) in the ventrorostral subregion of the left and right PMd, and both activated regions overlapped in many areas (light purple); (2) activation related to the transformation of a goal into an action in a rostral subregion of the left PMd (green); (3) activation related to action plan specification in a dorsocaudal subregion of the left PMd (yellow); and (4) activation related to action preparation in a caudal subregion of the left PMd (red). These subregions were adjacent to each other, except for the rostral subregion. These findings demonstrate that there are functional subregions within the PMd in humans with regard to achieving goal-directed motor behavior in a step-by-step fashion, and the subregions make a functional gradient in terms of cognitive to action processes along the rostral-caudal axis.

The activated areas identified in the present study are considered as effector-independent representations. In our previous research in monkeys, we recorded neuronal activity from only one hemisphere. By contrast, the present study has the advantage of being able to examine the bilateral hemispheres using fMRI and examine activation in an effector-independent manner. The present data suggest that the left PMd plays more crucial roles in goal-directed behavior than the right PMd, irrespective of which hand is used. This is plausible from a line of evidence showing that the left PMd plays an important role in movement selection cued by arbitrary stimuli and abstract cognitive functions (Callaert et al., 2011; Genon et al., 2018, 2017; Hanakawa et al., 2006; Rushworth et al., 2003, 1998; Schluter et al., 1998).

### 4.5. Possibility of other interpretations

One might suppose that the goal- or action-related activation observed in the present study reflects spatial attention or saccadic eye movements because several studies have shown that a certain portion of the PMd is involved in spatial attention (Boussaoud, 2001; Lebedev and Wise, 2001) or eye movements (Fujii et al., 2000; Kurata, 2017). However, in the present study, all of the stimuli were presented at the center of the screen and the participants were required to fixate on the fixation point at the center of the screen during the delay period before the appearance of the door cue. In addition, the participants did not have to attend to any spaces because they did not decide the action at that time. After the door cue was presented, the participants prepared a movement. It cannot be denied that spatial attention was included in the processes of motor preparation. However, because the proportion of movements to the right and left was identical for the *VM-go* and *VG-go conditions*, spatial biases were counterbalanced. Therefore, although we did not monitor eye movements, the activation observed in the present study is unlikely to reflect spatial attention.

Another line of evidence revealed that frontal lobe activation was correlated with response inhibition. The behavioral task of the present

study adopted a type of the Go/No-go task, which is a paradigm frequently used to measure response inhibition. Half of the trials in each *VM* and *VG condition* were in the Go condition and the other half were in the No-go condition, in which the participants had to inhibit their response. Therefore, we identified the brain regions that were activated in relation to response inhibition (Fig. S1 and Table S2), which was determined by the conjunction of the activity of the *VG conditions* (*VG-no-go – VG-go*) and that of the *VM conditions* (*VM-no-go – VM-go*) during the door cue period. Analysis revealed regions of significant activation in the bilateral dorsolateral prefrontal cortex, bilateral anterior cingulate cortex, bilateral insula, bilateral pre-SMA, left caudate, right PMv, bilateral M1, bilateral S1, bilateral SMG and superior temporal gyrus, bilateral cerebellum, and bilateral occipital regions (Fig. S1 and Table S2; $p < 0.05$ corrected at the cluster level). These results are consistent with the previous findings in terms of Go/No-go tasks (Hester et al., 2004; Schmidt et al., 2020; Simmonds et al., 2008). Moreover, previous findings indicate that the PMd plays an essential role in response inhibition (Battaglia-Mayer et al., 2014; Kalaska and Crammond, 1995; Levy and Wagner, 2011; Mirabella et al., 2011; Watanabe, 1986). However, we did not find activation in the PMd of both hemispheres (Fig. S1 and Table S2). One possible cause of this discrepancy could be the characteristics of the visuo-goal paradigm used in the present study; in the behavioral task, the participants were required to make a decision on what to do and make a Go/No-go decision simultaneously, which was not a pure response inhibition process.

### 4.6. Limitations and future directions

In the present study, we found the involvement of the bilateral PMd in a step-by-step process of goal-directed motor behavior. However, the present study has some limitations. First, we compared activation related to conditional visuomotor and visuo-goal mapping, but did not study direct visuomotor mapping. In rule-based visuomotor and visuo-goal mapping, a visual signal is mapped onto either an action or a goal in an arbitrary manner. However, in other situations such as reaching out and grasping a coffee cup, a visual stimulus can be the target itself (i.e., the coffee cup). In these cases, a visual signal is converted directly into a motor signal (direct or “standard” visuomotor mapping). Therefore, there are at least three behavioral control mechanisms based on visual cues (i.e., standard and conditional visuomotor mapping and conditional visuo-goal mapping). Further study is needed to compare directly the neural mechanisms between these three behavioral modes. Second, in the present and previous studies, the functional involvement of the parietal cortex in conditional visuo-goal and visuomotor behavior was not examined in detail. We found activation related to conditional visuomotor or visuo-goal mapping in parietal regions such as the SMG and AG. Our previous single-unit studies related to goal-directed behavior focused on the frontal regions (Nakayama et al., 2016, 2008; Yamagata et al., 2012, 2009), basal ganglia (Arimura et al., 2013), and thalamic reticular nucleus (Saga et al., 2017). As mentioned earlier, the parietal cortex may play a key role in conditional visuomotor and visuo-goal behavior. In the future, it would be of interest to study neuronal activity recorded from the parietal association areas, which will clarify the differential involvement of the frontal and parietal cortices in conditional visuomotor and visuo-goal behavior. Third, we did not examine the differences in behavior between the visuomotor and visuo-goal conditions. In the behavioral task of the present study, sufficient time was allotted between the appearance of the door cue and the appearance of the Go signal (door cue period), and the participants were required to respond within 1 s after the appearance of the Go signal. This paradigm allowed us to examine the neural representation of the preparation processes. Conversely, it cannot be used to investigate the behavioral differences between visuomotor and visuo-goal behavior. Visuo-goal behavior is considered to have a higher cognitive load than visuomotor behavior. Therefore, if a reaction time paradigm is adopted, we would expect to see behavioral differences, such as reaction time and response accuracy, between the two types of behavior. Further studies are needed to clarify the differences between visuomotor and visuo-goal behavior. Finally, the activation related to the transformation of a goal into an action was identified with small volume correction, whereas the other activated areas were identified with whole brain analysis. This may suggest that the contribution of the PMd to the transformation of a goal into an action is smaller than that of the other planning processes. Related to the discussion in the previous point, a reaction time paradigm would be useful to study the transformation processes in more detail. To examine the neural and behavioral differences between visuomotor and visuo-goal behavior, the contribution of the PMd to the transformation processes should be clarified.

### 4.7. Conclusions

In the present study, we examined the contributions of the PMd to conditional visuomotor and visuo-goal behavior in humans. We created a new visuo-goal task to investigate the step-by-step planning processes underlying visuomotor and visuo-goal behavior by using fMRI. We identified four different portions of the bilateral PMd that were activated during each of the planning processing steps. Conditional visuomotor and visuo-goal mapping were represented in the ventrorostral subregion of the bilateral PMd, action plan specification was represented in the dorsocaudal subregion of the left PMd, transformation of a goal into an action was represented in the rostral subregion of the left PMd, and action preparation map was represented by caudal subregions as well as the ventrorostral subregion of the bilateral PMd and bilateral M1. The activated areas related to each process were generally spatially separated from each other, but they overlapped partially. These findings revealed that there is a functional rostral-to-caudal gradient within the PMd in humans for achieving goal-directed behavior.

## Data availability statement

The data that support the findings of this study are openly available in OpenNeuro at https://openneuro.org/datasets/ds004056, doi:10.18112/openneuro.ds004056.

## Declaration of Competing Interest

None.

## Credit authorship contribution statement

**Yoshihisa Nakayama:** Conceptualization, Methodology, Software, Validation, Formal analysis, Investigation, Data curation, Writing – original draft, Writing – review & editing, Visualization, Project administration, Funding acquisition. **Sho K. Sugawara:** Conceptualization, Methodology, Software, Validation, Formal analysis, Investigation, Data curation, Writing – original draft, Writing – review & editing, Visualization. **Masaki Fukunaga:** Investigation, Data curation, Writing – review & editing. **Yuki H. Hamano:** Investigation, Data curation. **Norihiro Sadato:** Conceptualization, Methodology, Validation, Writing – review & editing, Supervision, Project administration, Funding acquisition. **Yukio Nishimura:** Conceptualization, Validation, Writing – review & editing, Supervision, Funding acquisition.

## Acknowledgments

We are grateful to Dr. E. Hoshi for helpful discussions and comments. We also thank Drs. E. J. Auerbach, E. Yacoub, and S. Moeller for providing the SMS EPI sequences, Dr. H-P. Fautz for providing the sequences for pre-scanning adjustment on 7T MRI, and the members of our laboratory for their support.

## Funding

This work was supported by a JSPS KAKENHI Grant-in-Aid for Scientific Research (C) (19K03377, to Y. Nakayama), Challenging Research (Exploratory) (18K19767, to Y. Nakayama and Y. Nishimura), Young Scientists (B) (JP16K17369, to Y. Nakayama), and the Cooperative Study Program of the National Institute for Physiological Sciences (17A042, 18A005, 19A005, and 20A008, to Y. Nakayama).

## Supplementary materials

Supplementary material associated with this article can be found, in the online version, at doi:10.1016/j.neuroimage.2022.119221.

## References

Abe, M., Hanakawa, T., 2009. Functional coupling underlying motor and cognitive functions of the dorsal premotor cortex. Behav. Brain Res. 198, 13–23. doi:10.1016/j.bbr.2008.10.046.

Alexander, G.E., Crutcher, M.D., 1990. Preparation for movement: neural representations of intended direction in three motor areas of the monkey. J. Neurophysiol. 64, 133–150. doi:10.1152/jn.1990.64.1.133.

Alexander, G.E., DeLong, M.R., Strick, P.L., 1986. Parallel organization of functionally segregated circuits linking basal ganglia and cortex. Annu. Rev. Neurosci. 9, 357–381. doi:10.1146/annurev.ne.09.030186.002041.

Alexander, M.P., Baker, E., Naeser, M.A., Kaplan, E., Palumbo, C., 1992. Neuropsychological and neuroanatomical dimensions of ideomotor apraxia. Brain 115, 87–107. doi:10.1093/brain/115.1.87.

Amiez, C., Kostopoulos, P., Champod, A.S., Petrides, M., 2006. Local morphology predicts functional organization of the dorsal premotor region in the human brain. J. Neurosci. 26, 2724–2731. doi:10.1523/jneurosci.4739-05.2006.

Andersson, J.L.R., Skare, S., Ashburner, J., 2003. How to correct susceptibility distortions in spin-echo echo-planar images: application to diffusion tensor imaging. Neuroimage 20, 870–888. doi:10.1016/s1053-8119(03)00336-7.

Apicella, P., Scarnati, E., Ljungberg, T., Schultz, W., 1992. Neuronal activity in monkey striatum related to the expectation of predictable environmental events. J. Neurophysiol. 68, 945–960. doi:10.1152/jn.1992.68.3.945.

Arimura, N., Nakayama, Y., Yamagata, T., Tanji, J., Hoshi, E., 2013. Involvement of the globus pallidus in behavioral goal determination and action specification. J. Neurosci. 33, 13639–13653. doi:10.1523/jneurosci.1620-13.2013.

Badre, D., D'Esposito, M., 2009. Is the rostro-caudal axis of the frontal lobe hierarchical? Nat. Rev. Neurosci. 10, 659–669. doi:10.1038/nrn2667.

Badre, D., Kayser, A.S., D'Esposito, M., 2010. Frontal cortex and the discovery of abstract action rules. Neuron 66, 315–326. doi:10.1016/j.neuron.2010.03.025.

Badre, D., Nee, D.E., 2018. Frontal cortex and the hierarchical control of behavior. Trends Cogn. Sci. 22, 170–188. doi:10.1016/j.tics.2017.11.005.

Battaglia-Mayer, A., Buiatti, T., Caminiti, R., Ferraina, S., Lacquaniti, F., Shallice, T., 2014. Correction and suppression of reaching movements in the cerebral cortex: physiological and neuropsychological aspects. Neurosci. Biobehav. Rev. 42, 232–251. doi:10.1016/j.neubiorev.2014.03.002.

Bollmann, S., Puckett, A.M., Cunnington, R., Barth, M., 2018. Serial correlations in single-subject fMRI with sub-second TR. Neuroimage 166, 152–166. doi:10.1016/j.neuroimage.2017.10.043.

Boussaoud, D., 2001. Attention versus intention in the primate premotor cortex. Neuroimage 14, S40–S45. doi:10.1006/nimg.2001.0816.

Boussaoud, D., Barth, T.M., Wise, S.P., 1993. Effects of gaze on apparent visual responses of frontal cortex neurons. Exp. Brain Res. 93, 423–434. doi:10.1007/bf00229358.

Boussaoud, D., Wise, S.P., 1993. Primate frontal cortex: effects of stimulus and movement. Exp. Brain Res. 95, 28–40. doi:10.1007/bf00229651.

Buxbaum, L.J., Randerath, J., 2018. Limb apraxia and the left parietal lobe. Handb. Clin. Neurol. 151, 349–363. doi:10.1016/b978-0-444-63622-5.00017-6.

Callaert, D.V., Vercauteren, K., Peeters, R., Tam, F., Graham, S., Swinnen, S.P., Sunaert, S., Wenderoth, N., 2011. Hemispheric asymmetries of motor versus nonmotor processes during (visuo)motor control. Hum. Brain Mapp. 32, 1311–1329. doi:10.1002/hbm.21110.

Chou, T.L., Booth, J.R., Burman, D.D., Bitan, T., Bigio, J.D., Lu, D., Cone, N.E., 2006. Developmental changes in the neural correlates of semantic processing. Neuroimage 29, 1141–1149. doi:10.1016/j.neuroimage.2005.09.064.

Cisek, P., Kalaska, J.F., 2005. Neural correlates of reaching decisions in dorsal premotor cortex: specification of multiple direction choices and final selection of action. Neuron 45, 801–814. doi:10.1016/j.neuron.2005.01.027.

Corbin, N., Todd, N., Friston, K.J., Callaghan, M.F., 2018. Accurate modeling of temporal correlations in rapidly sampled fMRI time series. Hum. Brain Mapp. 39, 3884–3897. doi:10.1002/hbm.24218.

Deschamps, I., Baum, S.R., Gracco, V.L., 2014. On the role of the supramarginal gyrus in phonological processing and verbal working memory: evidence from rTMS studies. Neuropsychologia 53, 39–46. doi:10.1016/j.neuropsychologia.2013.10.015.

Evarts, E.V., 1964. Temporal patterns of discharge of pyramidal tract neurons during sleep and waking in the monkey. J. Neurophysiol. 27, 152–171. doi:10.1152/jn.1964.27.2.152.

Fan, L., Li, H., Zhuo, J., Zhang, Y., Wang, J., Chen, L., Yang, Z., Chu, C., Xie, S., Laird, A.R., Fox, P.T., Eickhoff, S.B., Yu, C., Jiang, T., 2016. The human brainnetome atlas: a new brain atlas based on connectional architecture. Cereb. Cortex 26, 3508–3526. doi:10.1093/cercor/bhw157.

Friston, K.J., Glaser, D.E., Henson, R.N.A., Kiebel, S., Phillips, C., Ashburner, J., 2002. Classical and bayesian inference in neuroimaging: applications. Neuroimage 16, 484–512. doi:10.1006/nimg.2002.1091.

Friston, K.J., Holmes, A., Poline, J.B., Price, C.J., Frith, C.D., 1996. Detecting activations in PET and fMRI: levels of inference and power. Neuroimage 4, 223–235. doi:10.1006/nimg.1996.0074.

Friston, K.J., Jezzard, P., Turner, R., 1994. Analysis of functional MRI time-series. Hum. Brain Mapp. 1, 153–171. doi:10.1002/hbm.460010207.

Fujii, N., Mushiake, H., Tanji, J., 2000. Rostrocaudal distinction of the dorsal premotor area based on oculomotor involvement. J. Neurophysiol. 83, 1764–1769. doi:10.1152/jn.2000.83.3.1764.

Genon, S., Li, H., Fan, L., Müller, V.I., Cieslik, E.C., Hoffstaedter, F., Reid, A.T., Langner, R., Grefkes, C., Fox, P.T., Moebus, S., Caspers, S., Amunts, K., Jiang, T., Eickhoff, S.B., 2017. The right dorsal premotor mosaic: organization, functions, and connectivity. Cereb. Cortex 27, 2095–2110. doi:10.1093/cercor/bhw065.

Genon, S., Reid, A., Li, H., Fan, L., Müller, V.I., Cieslik, E.C., Hoffstaedter, F., Langner, R., Grefkes, C., Laird, A.R., Fox, P.T., Jiang, T., Amunts, K., Eickhoff, S.B., 2018. The heterogeneity of the left dorsal premotor cortex evidenced by multimodal connectivity-based parcellation and functional characterization. Neuroimage 170, 400–411. doi:10.1016/j.neuroimage.2017.02.034.

Glasser, M.F., Coalson, T.S., Robinson, E.C., Hacker, C.D., Harwell, J., Yacoub, E., Ugurbil, K., Andersson, J., Beckmann, C.F., Jenkinson, M., Smith, S.M., Essen, D.C.V., 2016. A multi-modal parcellation of human cerebral cortex. Nature 536, 171–178. doi:10.1038/nature18933.

Glasser, M.F., Sotiropoulos, S.N., Wilson, J.A., Coalson, T.S., Fischl, B., Andersson, J.L., Xu, J., Jbabdi, S., Webster, M., Polimeni, J.R., Essen, D.C.V., Jenkinson, M.Consortium, for the W.M.H., 2013. The minimal preprocessing pipelines for the human connectome project. Neuroimage 80, 105–124. doi:10.1016/j.neuroimage.2013.04.127.

Grafton, S.T., Hazeltine, E., Ivry, R.B., 1998. Abstract and effector-specific representations of motor sequences identified with PET. J. Neurosci. 18, 9420–9428. doi:10.1523/jneurosci.18-22-09420.1998.

Greve, D.N., Fischl, B., 2009. Accurate and robust brain image alignment using boundary-based registration. Neuroimage 48, 63–72. doi:10.1016/j.neuroimage.2009.06.060.

Halsband, U., Passingham, R.E., 1985. Premotor cortex and the conditions for movement in monkeys (Macaca fascicularis). Behav. Brain Res. 18, 269–277. doi:10.1016/0166-4328(85)90035-x.

Hanakawa, T., Honda, M., Zito, G., Dimyan, M.A., Hallett, M., 2006. Brain activity during visuomotor behavior triggered by arbitrary and spatially constrained cues: an fMRI study in humans. Exp. Brain Res. 172, 275–282. doi:10.1007/s00221-005-0336-z.

Heilman, K.M., Rothi, L.J., Valenstein, E., 1982. Two forms of ideomotor apraxia. Neurology 32, 342. doi:10.1212/wnl.32.4.342.

Hester, R., Fassbender, C., Garavan, H., 2004. Individual differences in processing: a review and reanalysis of three event-related fMRI studies using the GO/NOGO task. Cereb. Cortex 14, 986–994. doi:10.1093/cercor/bhh059.

Holmes, A.P., Friston, K.J., 1998. Generalisability, random effects & population inference. Neuroimage 7, S754. doi:10.1016/s1053-8119(18)31587-8.

Kalaska, J.F., 2009. Progress in motor control, a multidisciplinary perspective. Adv. Exp. Med. Biol. 629, 139–178. doi:10.1007/978-0-387-77064-2_8.

Kalaska, J.F., Crammond, D.J., 1995. Deciding not to GO: neuronal correlates of response selection in a GO/NOGO task in primate premotor and parietal cortex. Cereb. Cortex 5, 410–428. doi:10.1093/cercor/5.5.410.

Kamali, A., Flanders, A.E., Brody, J., Hunter, J.V., Hasan, K.M., 2014. Tracing superior longitudinal fasciculus connectivity in the human brain using high resolution diffusion tensor tractography. Brain Struct. Funct. 219, 269–281. doi:10.1007/s00429-012-0498-y.

Kemmerer, D., Rudrauf, D., Manzel, K., Tranel, D., 2012. Behavioral patterns and lesion sites associated with impaired processing of lexical and conceptual knowledge of actions. Cortex 48, 826–848. doi:10.1016/j.cortex.2010.11.001.

Koelsch, S., Schulze, K., Sammler, D., Fritz, T., Müller, K., Gruber, O., 2009. Functional architecture of verbal and tonal working memory: an FMRI study. Hum. Brain Mapp. 30, 859–873. doi:10.1002/hbm.20550.

Kurata, K., 2017. Movement-related activity in the periarcuate cortex of monkeys during coordinated eye and hand movements. J. Neurophysiol. 118, 3293–3310. doi:10.1152/jn.00279.2017.

Kurata, K., Hoffman, D.S., 1994. Differential effects of muscimol microinjection into dorsal and ventral aspects of the premotor cortex of monkeys. J. Neurophysiol. 71, 1151–1164. doi:10.1152/jn.1994.71.3.1151.

Lebedev, M.A., Wise, S.P., 2001. Tuning for the orientation of spatial attention in dorsal premotor cortex. Eur. J. Neurosci. 13, 1002–1008. doi:10.1046/j.0953-816x.2001.01457.x.

Levy, B.J., Wagner, A.D., 2011. Cognitive control and right ventrolateral prefrontal cortex: reflexive reorienting, motor inhibition, and action updating. Ann. N.Y. Acad. Sci. 1224, 40–62. doi:10.1111/j.1749-6632.2011.05958.x.

Mai, J.K., Majtanik, M., Paxinos, G., 2015. Atlas of the Human Brain, (4th ed.) Academic Press, Amsterdam.

Martino, J., Hamer, P.C.D.W., Berger, M.S., Lawton, M.T., Arnold, C.M., Lucas, E.M.d.e., Duffau, H., 2013. Analysis of the subcomponents and cortical terminations of the perisylvian superior longitudinal fasciculus: a fiber dissection and DTI tractography study. Brain Struct. Funct. 218, 105–121. doi:10.1007/s00429-012-0386-5.

Mirabella, G., Pani, P., Ferraina, S., 2011. Neural correlates of cognitive control of reaching movements in the dorsal premotor cortex of rhesus monkeys. J. Neurophysiol. 106, 1454–1466. doi:10.1152/jn.00995.2010.

Moeller, S., Yacoub, E., Olman, C.A., Auerbach, E., Strupp, J., Harel, N., Uğurbil, K., 2010. Multiband multislice GE-EPI at 7 tesla, with 16-fold acceleration using partial paral-

lel imaging with application to high spatial and temporal whole-brain fMRI. Magn. Reson. Med. 63, 1144–1153. doi:10.1002/mrm.22361.
Mugler, J.P., Bao, S., Mulkern, R.V., Guttmann, C.R.G., Robertson, R.L., Jolesz, F.A., Brookeman, J.R., 2000. Optimized single-slab three-dimensional spin-echo MR imaging of the brain. Radiology 216, 891–899. doi:10.1148/radiology.216.3.r00au46891.
Mugler, J.P., Brookeman, J.R., 1990. Three-dimensional magnetization-prepared rapid gradient-echo imaging (3D MP RAGE). Magn. Reson. Med. 15, 152–157. doi:10.1002/mrm.1910150117.
Nakayama, Y., Yamagata, T., Hoshi, E., 2016. Rostrocaudal functional gradient among the pre-dorsal premotor cortex, dorsal premotor cortex and primary motor cortex in goal-directed motor behaviour. Eur. J. Neurosci. 43, 1569–1589. doi:10.1111/ejn.13254.
Nakayama, Y., Yamagata, T., Tanji, J., Hoshi, E., 2008. Transformation of a virtual action plan into a motor plan in the premotor cortex. J. Neurosci. 28, 10287–10297. doi:10.1523/jneurosci.2372-08.2008.
Oldfield, R.C., 1971. The assessment and analysis of handedness: the Edinburgh inventory. Neuropsychologia 9, 97–113. doi:10.1016/0028-3932(71)90067-4.
Passingham, R.E., 1993. The Frontal Lobes and Voluntary Action. Oxford University Press, Oxford, UK.
Petrides, M., 1986. The effect of periarcuate lesions in the monkey on the performance of symmetrically and asymmetrically reinforced visual and auditory go, no-go tasks. J. Neurosci. 6, 2054–2063. doi:10.1523/jneurosci.06-07-02054.1986.
Picard, N., Strick, P.L., 2001. Imaging the premotor areas. Curr. Opin. Neurobiol. 11, 663–672. doi:10.1016/s0959-4388(01)00266-5.
Poldrack, R.A., 2007. Region of interest analysis for fMRI. Soc. Cogn. Affect. Neurosci. 2, 67–70. doi:10.1093/scan/nsm006.
Rushworth, M.F.S., Behrens, T.E.J., Johansen-Berg, H., 2006. Connection patterns distinguish 3 regions of human parietal cortex. Cereb. Cortex 16, 1418–1430. doi:10.1093/cercor/bhj079.
Rushworth, M.F.S., Johansen-Berg, H., Göbel, S.M., Devlin, J.T., 2003. The left parietal and premotor cortices: motor attention and selection. Neuroimage 20, S89–S100. doi:10.1016/j.neuroimage.2003.09.011.
Rushworth, M.F.S., Nixon, P.D., Wade, D.T., Renowden, S., Passingham, R.E., 1998. The left hemisphere and the selection of learned actions. Neuropsychologia 36, 11–24. doi:10.1016/s0028-3932(97)00101-2.
Saga, Y., Nakayama, Y., Inoue, K., Yamagata, T., Hashimoto, M., Tremblay, L., Takada, M., Hoshi, E., 2017. Visuomotor signals for reaching movements in the rostro-dorsal sector of the monkey thalamic reticular nucleus. Eur. J. Neurosci. 45, 1186–1199. doi:10.1111/ejn.13421.
Sakai, K.L., 2005. Language acquisition and brain development. Science 310, 815–819. doi:10.1126/science.1113530.
Salmon, E., Linden, M.V.der, Collette, F., Delfiore, G., Maquet, P., Degueldre, C., Luxen, A., Franck, G., 1996. Regional brain activity during working memory tasks. Brain 119, 1617–1625. doi:10.1093/brain/119.5.1617.
Schluter, N.D., Rushworth, M.F., Passingham, R.E., Mills, K.R., 1998. Temporary interference in human lateral premotor cortex suggests dominance for the selection of movements. A study using transcranial magnetic stimulation. Brain 121, 785–799. doi:10.1093/brain/121.5.785.
Schmidt, C.C., Timpert, D.C., Arend, I., Vossel, S., Fink, G.R., Henik, A., Weiss, P.H., 2020. Control of response interference: caudate nucleus contributes to selective inhibition. Sci. Rep. 10, 20977. doi:10.1038/s41598-020-77744-1.
Simmonds, D.J., Pekar, J.J., Mostofsky, S.H., 2008. Meta-analysis of Go/No-go tasks demonstrating that fMRI activation associated with response inhibition is task-dependent. Neuropsychologia 46, 224–232. doi:10.1016/j.neuropsychologia.2007.07.015.
Simon, S.R., Meunier, M., Piettre, L., Berardi, A.M., Segebarth, C.M., Boussaoud, D., 2002. Spatial attention and memory versus motor preparation: premotor cortex involvement as revealed by fMRI. J. Neurophysiol. 88, 2047–2057. doi:10.1152/jn.2002.88.4.2047.
Stoeckel, C., Gough, P.M., Watkins, K.E., Devlin, J.T., 2009. Supramarginal gyrus involvement in visual word recognition. Cortex 45, 1091–1096. doi:10.1016/j.cortex.2008.12.004.
Takada, M., Tokuno, H., Nambu, A., Inase, M., 1998. Corticostriatal projections from the somatic motor areas of the frontal cortex in the macaque monkey: segregation versus overlap of input zones from the primary motor cortex, the supplementary motor area, and the premotor cortex. Exp. Brain Res. 120, 114–128. doi:10.1007/s002210050384.
Takahara, D., Inoue, K., Hirata, Y., Miyachi, S., Nambu, A., Takada, M., Hoshi, E., 2012. Multisynaptic projections from the ventrolateral prefrontal cortex to the dorsal premotor cortex in macaques – anatomical substrate for conditional visuomotor behavior. Eur. J. Neurosci. 36, 3365–3375. doi:10.1111/j.1460-9568.2012.08251.x.
Tanji, J., Evarts, E.V., 1976. Anticipatory activity of motor cortex neurons in relation to direction of an intended movement. J. Neurophysiol. 39, 1062–1068. doi:10.1152/jn.1976.39.5.1062.
Toni, I., Rowe, J., Stephan, K.E., Passingham, R.E., 2002. Changes of cortico-striatal effective connectivity during visuomotor learning. Cereb. Cortex 12, 1040–1047. doi:10.1093/cercor/12.10.1040.
Toni, I., Rushworth, M.F., Passingham, R.E., 2001. Neural correlates of visuomotor associations. Exp. Brain Res. 141, 359–369. doi:10.1007/s002210100877.
Toni, I., Schluter, N.D., Josephs, O., Friston, K., Passingham, R.E., 1999. Signal-, set- and movement-related activity in the human brain: an event-related fMRI study. Cereb. Cortex 9, 35–49. doi:10.1093/cercor/9.1.35.
Tranel, D., Kemmerer, D., Adolphs, R., Damasio, H., Damasio, A.R., 2003. Neural correlates of conceptual knowledge for actions. Cogn. Neuropsychol. 20, 409–432. doi:10.1080/02643290244000248.
Uddin, L.Q., Supekar, K., Amin, H., Rykhlevskaia, E., Nguyen, D.A., Greicius, M.D., Menon, V., 2010. Dissociable connectivity within human angular gyrus and intraparietal sulcus: evidence from functional and structural connectivity. Cereb. Cortex 20, 2636–2646. doi:10.1093/cercor/bhq011.
Wang, X., Pathak, S., Stefaneanu, L., Yeh, F.C., Li, S., Fernandez-Miranda, J.C., 2016. Subcomponents and connectivity of the superior longitudinal fasciculus in the human brain. Brain Struct. Funct. 221, 2075–2092. doi:10.1007/s00429-015-1028-5.
Watanabe, M., 1986. Prefrontal unit activity during delayed conditional Go/No-go discrimination in the monkey. II. Relation to Go and No-go responses. Brain Res. 382, 15–27. doi:10.1016/0006-8993(86)90105-8.
Wheaton, L.A., Hallett, M., 2007. Ideomotor apraxia: a review. J. Neurol. Sci. 260, 1–10. doi:10.1016/j.jns.2007.04.014.
Worsley, K.J., Friston, K.J., 1995. Analysis of fMRI time-series revisited—again. Neuroimage 2, 173–181. doi:10.1006/nimg.1995.1023.
Yamagata, T., Nakayama, Y., Tanji, J., Hoshi, E., 2012. Distinct information representation and processing for goal-directed behavior in the dorsolateral and ventrolateral prefrontal cortex and the dorsal premotor cortex. J. Neurosci. 32, 12934–12949. doi:10.1523/jneurosci.2398-12.2012.
Yamagata, T., Nakayama, Y., Tanji, J., Hoshi, E., 2009. Processing of visual signals for direct specification of motor targets and for conceptual representation of action targets in the dorsal and ventral premotor cortex. J. Neurophysiol. 102, 3280–3294. doi:10.1152/jn.00452.2009.
Yamamoto, T., Fukunaga, M., Sugawara, S.K., Hamano, Y.H., Sadato, N., 2021. Quantitative evaluations of geometrical distortion corrections in cortical surface-based analysis of high-resolution functional MRI data at 7T. J. Magn. Reson. Imaging 53, 1220–1234. doi:10.1002/jmri.27420.